Supramolecular Chemistry

International Edition: DOI: 10.1002/anie.201602894
German Edition: DOI: 10.1002/ange.201602894

Stepwise Unfolding of Single-Chain Nanoparticles by Chemically Triggered Gates

Tobias S. Fischer, David Schulze-Sünninghausen, Burkhard Luy, Ozcan Altintas, and Christopher Barner-Kowollik**

Abstract: *The orthogonal, stepwise, and order-independent unfolding of single-chain nanoparticles (SCNPs) is introduced as a key step towards actively controlling the folding dynamics of SCNPs. The SCNPs are compacted by multiple hydrogen bonds and host–guest interactions. Well-defined diblock (AB) and tetrablock (ABCD) copolymers are equipped with orthogonal recognition motifs via modular ligation along the lateral chain. Initially, single-chain folding of the diblock copolymer was induced by the host–guest complexation of benzo-21-crown-7 (B21C7, host) and a secondary ammonium salt (AS, guest), representing an efficient avenue for single-chain collapse. Next, both orthogonal Hamilton wedge (HW) and cyanuric acid (CA) as well as B21C7–AS motifs were employed to generate SCNPs based on the ABCD polymer system. Subsequently, the stepwise dual-gated and order-independent unfolding of the SCNPs was investigated by the addition of external stimuli. The folding and unfolding were explored by 1D ^{1}H NMR spectroscopy, dynamic light scattering (DLS), and diffusion-ordered NMR spectroscopy (DOSY).*

Complex functional biomacromolecular entities such as proteins and enzymes are finely controlled macromolecules. However, nature's exquisite degree of control is beyond the reach of contemporary synthetic macromolecular chemistry. The conformation of biopolymers is controlled by reversible self-folding processes, typically driven by covalent or—in many cases—noncovalent interactions.[1–3] Proteins fold dynamically into more complex structures, such as α-helices and β-sheets. Intramolecular hydrogen bonds, aromatic stacking, and hydrophobic interactions typically stabilize the formed architectures.[4,5] The intramolecular folding of suitably functionalized synthetic polymer strands into compact single-chain nanoparticles is one actively explored avenue for mimicking natural analogues.[6,7] The field of single-chain folding is a growing area of polymer science and takes inspiration from nature's folding processes.[8–12] Well-defined functional polymers are accessible via the application of reversible deactivation radical polymerization (RDRP) techniques. By the combination of RDRP techniques with orthogonal polymer ligation protocols, it is possible to enable the folding of synthetic macromolecules through the interactions of specifically placed functionalities along the lateral polymer chain.[13–16] The resulting folded structures are mostly stabilized by noncovalent interactions,[5] such as hydrogen bonds,[17–19] π–π stacking,[20] host–guest interactions,[21,22] and metal complexation,[23,24] yet studies to trigger the defined unfolding of dynamic SCNPs are scarce.

We have recently focused on designing well-defined synthetic polymers carrying dynamically orthogonally operating complementary motifs that induce folding into a particular conformation. In the current study, we introduce a complementary motif for single-chain folding technology adopted from supramacromolecular chemistry and exploit it along with a known hydrogen-bond-driven collapse system to introduce a new class of SCNPs able to undergo dual-gated order-independent unfolding by independent chemical trigger signals (Scheme 1). SCNP unfolding has been explored before only by Meijer and co-workers in an elegant study, who—in contrast to the present study—forced the unfolding by atomic force microscopy (AFM)-based single-molecule force spectroscopy (SMFS).[25] Now, we add to the field of controlled unfolding by describing the first system that can be unfolded through the action of two independent chemical trigger signals.

We synthesized a highly defined tetrablock ABCD copolymer with orthogonal folding functionalities attached to specific block segments (hydrogen-bonding system and host–guest system). We subsequently studied the intramolecular folding of the host–guest complexation system, that is, the interaction of benzo-21-crown-7 (B21C7, host) with a secondary ammonium salt (AS, guest) (Scheme 2a). Wang and coworkers demonstrated the orthogonality of the Hamilton wedge/cyanuric acid (HW/CA) as well as B21C7–AS recognition motifs by NMR spectroscopic analysis of functional small molecules in the context of supramolecular polymer design.[26] The precursor block copolymers (AB- and ABCD-type) were synthesized via RAFT polymerization and characterized by 1D ^{1}H NMR spectroscopy and size-exclusion chromatography (SEC).[24] All synthetic details of the pre-

[*] T. S. Fischer, Dr. O. Altintas, Prof. C. Barner-Kowollik
Preparative Macromolecular Chemistry, Institut für Technische Chemie und Polymerchemie, Karlsruhe Institute of Technology (KIT)
Engesserstrasse 18, 76128 Karlsruhe (Germany)
E-mail: christopher.barner-kowollik@kit.edu
oezcan.altintas@kit.edu

T. S. Fischer, D. Schulze-Sünninghausen, Prof. B. Luy, Dr. O. Altintas, Prof. C. Barner-Kowollik
Institut für Biologische Grenzflächen
Karlsruhe Institute of Technology (KIT)
Hermann-von-Helmholtz-Platz 1,
76344 Eggenstein, Leopoldshafen (Germany)

D. Schulze-Sünninghausen, Prof. B. Luy
Institut für Organische Chemie
Karlsruhe Institute of Technology (KIT)
Fritz-Haber-Weg 6, 76131 Karlsruhe (Germany)

Supporting information for this article can be found under: http://dx.doi.org/10.1002/anie.201602894.

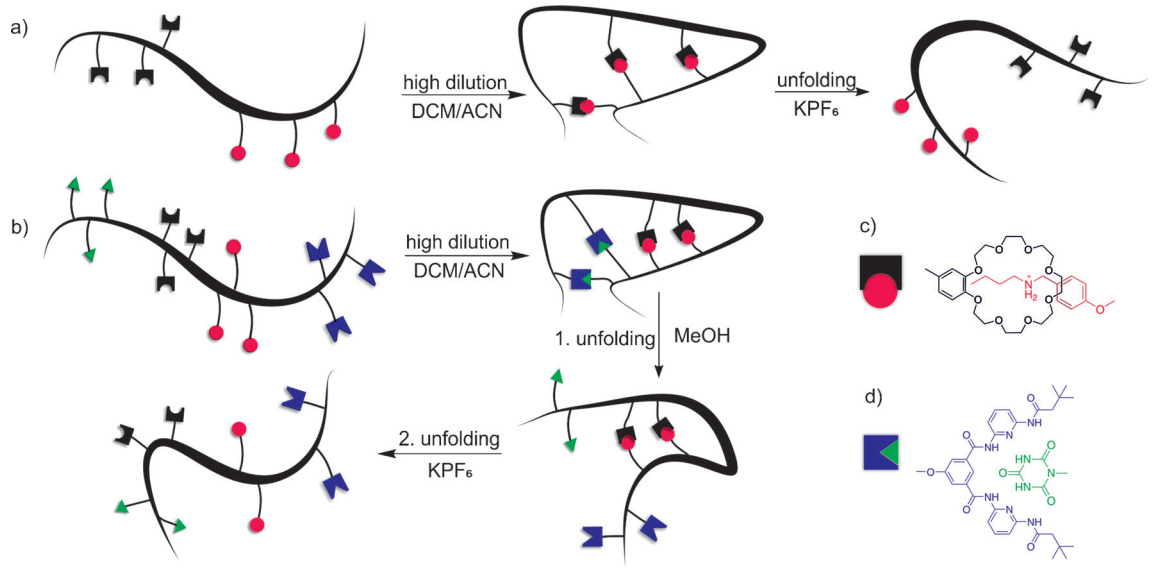

Scheme 1. a) Design of the initial diblock copolymer system bearing the host–guest folding motif (B21C7–AS), followed by the folding/unfolding of the resulting SCNP. b) Design of the tetrablock copolymer systems featuring the orthogonal complementary folding motifs (HW, CA and B21C7, AS), followed by folding and the orthogonal stepwise unfolding. The indicated unfolding is independent of the order of addition of the stimuli (see text). c) Self-assembly of HW and CA via multiple hydrogen bonds. d) Self-assembly of B21C7 and AS units via host–guest complexation.

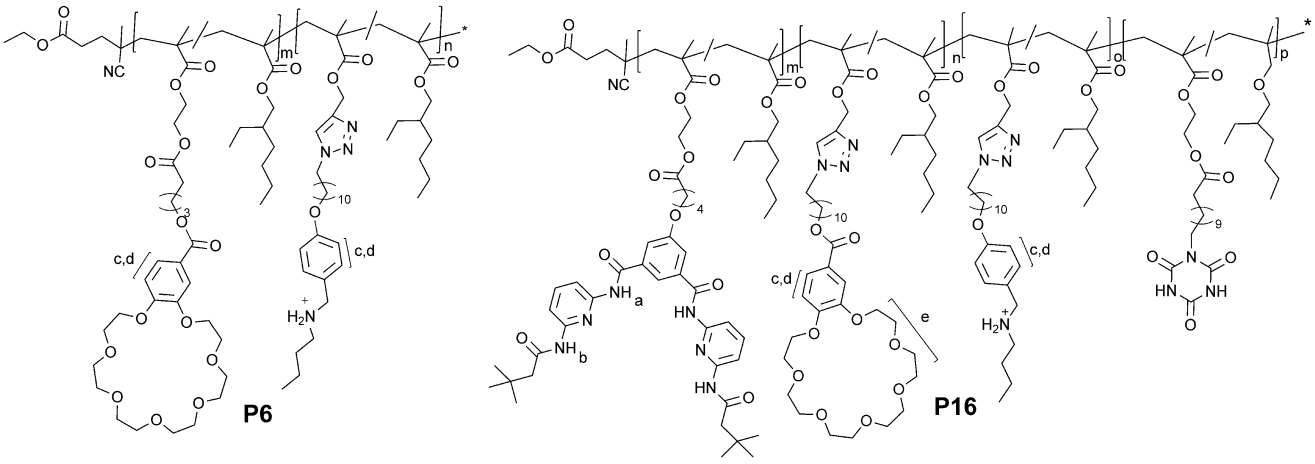

Scheme 2. a) Chemical structure and NMR assignments of the functionalized diblock copolymer **P6**. b) Chemical structure and NMR assignments of the functionalized tetrablock copolymer **P16**.

cursor block copolymers can be found in Figures S16–S28 in the Supporting Information (SI)). The well-defined block copolymers were functionalized with the respective complementary motifs after the removal of the RAFT agent.[27] Specifically, the acid-functional B21C7 **6** was reacted with the bromine functionality of the diblock copolymer **P2** and subsequently the boc-protected AS moiety **9** was attached via [3+2] copper-catalyzed azide–alkyne cycloaddition (CuAAC) (see Scheme S3) to afford polymer **P5**.[28] After the attachment of the B21C7 and protected AS functionalities to the diblock copolymer test system, the final diblock copolymer **P6** was obtained by deprotection of the AS moiety[29] (1D ^{1}H NMR spectra and SEC data for **P1**–**P5** can be found in the Figures S16 and S17). Subsequently, the tetrablock copolymer was prepared and postfunctionalized with the orthogonal folding units. The HW and CA recognition motifs were attached to the outer blocks A and D, while the B21C7–AS moieties were grafted to the inner blocks B and C (Scheme 2b). In a nucleophilic substitution reaction, the hydroxyl-functional HW **2** was reacted with the bromine functionality of **P10**. The azide-functional B21C7 **7** and protected AS **9** were orthogonally linked by [3+2] CuAAC (see Scheme S5). The CA moiety **3** was attached to the polymer **P14** via Steglich esterification,[30] before the boc protecting group of the AS moiety was removed and the final polymer **P16** was obtained. Molecular characteristics of the polymers are given in Table 1 (1D ^{1}H NMR spectra and SEC data for **P7**–**P15** can be found in Figures S27 and S28).

The characterization of dynamic SCNPs is not feasible with most common polymer characterization techniques as

Table 1: Characterization data for the di- and tetrablock copolymer synthesized by RAFT.[a]

Polymer	$M_{n,theo}$[b] [kDa]	$M_{n,SEC}$[c] [kDa]	$Đ$[c]	HW [mol%][d]	B21C7 [mol%][d]	AS [mol%][d]	CA [mol%][d]
P6	37.5	30.6	1.1	–	5.2	6.5	–
P16	65.9	64.8	1.2	5.2	5.5	6.0	2.4

[a] For the full molecular weight distributions (MWDs) refer to the Supporting Information (Figures S17 and S28). [b] Details of the calculation of $M_{n,theo}$ can be found in the Supporting Information. [c] Determined via SEC using THF as eluent, calibrated with pMMA standards. SEC analysis of **P6** and **P16** could not be performed due to the ionic nature of the polymers. Thus, SEC data of the block polymers of the previous step are provided. [d] Mol percentage of incorporated functional monomers in each block segment relative to the incorporated EHMA monomer of each block as determined via ^{1}H NMR spectroscopy by integration of the end groups and/or relative intensities of selected signals. The details of the calculations can be found in the Supporting Information.

noncovalent interactions are strongly affected by solvent, concentration, temperature, and pressure.[8,28] The formation of the hydrogen bonds of the HW/CA moieties[18] as well as the host–guest interaction is verified in the 1D ^{1}H NMR spectrum (Figure 1).[23,29,30]

The proton resonances **a** and **b** at 9.65 and 9.31 ppm are attributed to the amide protons of the HW (Figure 1), indicating the formation of hydrogen bonds between the HW and the CA recognition units.[18] The imide proton resonances in the range of 11–13 ppm of CA are in a coalescence regime, where the resonances of the bound NH protons are very broad, likely due to a strong exchange broadening (see also Figure S35).[3,34] Changes in the aromatic region at 6.9–7.7 ppm, resonances **c** and **d**, as well as the change of the CH_2 resonance **e** associated with the ethyleneoxy bridges of the B21C7 next to the phenol ring at 4.21 ppm indicate the interaction of the B21C7–AS moieties, as the chemical environment changes due to the host–guest interaction (Figure 1). Accordingly, unfolding events upon addition of methanol (MeOH), in order to weaken the HW/CA hydrogen bonds (resonances **a** and **b**), and KPF_6, causing the disruption of the B12C7/AS complex, can be directly monitored.

In the next step, the dual-gated and independent folding/unfolding behavior of the synthesized systems was evidenced by dynamic light scattering (DLS) and diffusion-ordered NMR spectroscopy (DOSY). The DLS-derived hydrodynamic diameters (D_h, see Figure 2a,b) of the folded and unfolded polymers **P6** and **P16** are listed in Table 2. As noted, the dissociation of the hydrogen-bonding system can be induced by addition of a competitive solvent such as methanol,[34] while the host–guest interaction can be disrupted by adding a simple potassium salt as the potassium cation is complexed stronger by B21C7 than the AS moiety.[33] The unfolding of the dual folding system in **P16** can be realized by first breaking the hydrogen bonds of HW/CA and subsequently the B21C7–AS interaction or vice versa (pathway independ-

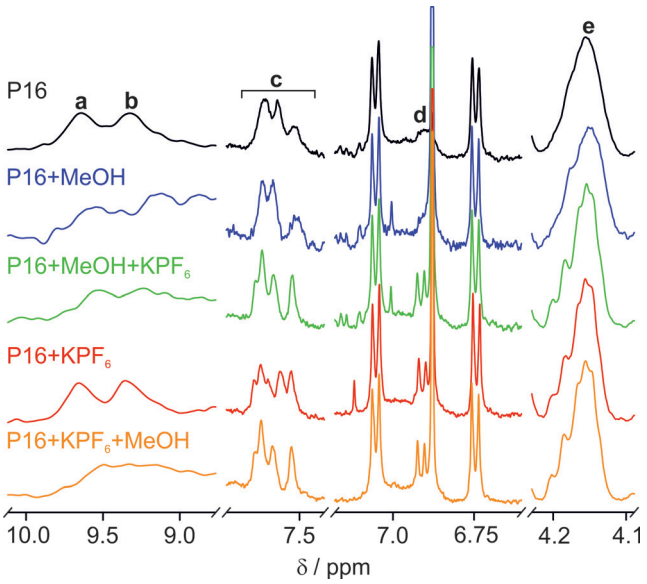

Figure 1. Relevant sections of the 1D ^{1}H NMR spectra for the unfolding of the tetrablock copolymer **P16**. Resonances labeled **a** and **b** indicate the interaction of the complementary motifs HW–CA, the resonances labeled **c**–**e** indicate the host–guest interaction of B21C7–AS. The assignments of the peaks can be found in Scheme 2. The orthogonal recognition units can be found in Scheme 1c,d.

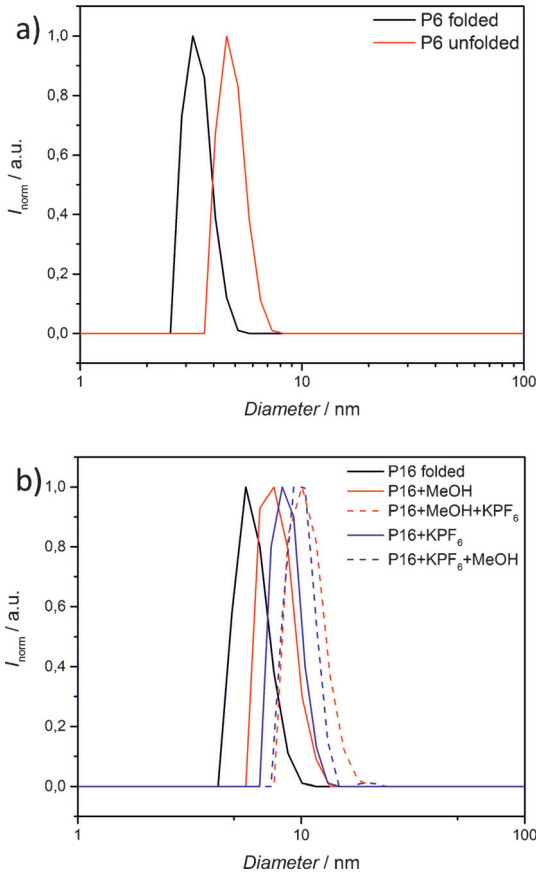

Figure 2. a) Dynamic light scattering (DLS) data (number distributions) for the folded and unfolded polymer **P6**. b) Dynamic light scattering (DLS) data (number distributions) for the folded and unfolded polymer **P16**. The hydrodynamic diameters (D_h) of the folded and unfolded polymers **P6** and **P16** are collated in Table 2.

Table 2: DLS and DOSY data for the folded and unfolded states of the di- and tetrablock copolymers **P6** and **P16**.

Polymer	$D_{h,DLS}$[a] [nm]	$D_{h,DOSY}$[b,c] [nm]
P6 folded	3.4	2.5
P6 unfolded	4.8	3.3
P16 folded	6.0	7.1
P16 + MeOH	7.9	8.7
P16 + MeOH + KPF	10.5	10.6
P16 + KPF_6	8.6	9.6
P16 + KPF_6 + MeOH	10.0	10.1

[a] The hydrodynamic diameter (D_h) determined by DLS in a mixture of DCM/acetonitrile (9:1, v/v) at 25 °C, $c_{polymer} = 2.5\ mg\,mL^{-1}$. [b] D_h obtained by DOSY experiments in a mixture of DCM/acetonitrile (9:1, v/v) at 25 °C, $c_{polymer} = 2.5\ mg\,mL^{-1}$, using the Stokes–Einstein equation for calculation. [c] For potential systematic errors in the single-exponential fit refer to the Supporting Information.

ence). Before the unfolding behavior of **P16** was investigated (see Figure 2b), the B21C7–AS motif in **P6** was tested to evidence the unfolding abilities of the system in a SCNP context (see Figure 2a). Herein we focus on the low-concentration regime,[3] as at low concentrations intramolecular folding occurs, while intermolecular aggregation dominates at higher concentrations.[3,22] The DLS data indicate a transition from intramolecular folding to the formation of intermolecular aggregates when going to higher concentrations. Starting at a concentration of approximately $8\ mg\,mL^{-1}$, intermolecular interactions dominate (cf. Figures S33 and S34). When an excess of KPF_6 (4 mg) is added to **P6** (2.5 mg in 1 mL solvent, DCM/acetonitrile 9:1, v/v), DLS indicates an increase in the hydrodynamic diameter of 1.4 nm from the folded to the unfolded state (Table 2, entries 1 and 2). Next, the orthogonal stepwise unfolding of the complementary recognition units in **P16** was investigated. Methanol (20 μL) was added to a solution of **P16**, upon which D_h increased by almost 2 nm (Table 2, entries 3 and 4). When KPF_6 is added, D_h increases again by almost 2 nm. Inverting the order of the added triggers leads to a similar increase in D_h based on DLS (Table 2, entries 6 and 7). Finally, the unfolding of **P6** and the orthogonal dissociation of the distinct motifs of **P16** were also studied by DOSY, which in essence provided the same results (see Table 2) as DLS in terms of changes in the hydrodynamic diameter, and thus strongly underpin the conclusion that **P16** indeed shows orthogonal and dual-gated unfolding independent of the order of the added triggers.

We have reported an advanced dual-gated orthogonal SCNP unfolding system based on a modular synthetic strategy towards well-defined block copolymers carrying orthogonal complementary binding motifs by a combination of RAFT polymerization and modular ligation. First, an AB-type diblock copolymer carrying the benzo-21-crown-7 (B21C7)/secondary ammonium salt (AS) host–guest system was explored in terms of its triggered unfolding behavior. Next, an ABCD-type tetrablock copolymer bearing dual orthogonal complementary folding motifs, that is, the hydrogen-bonding motif (Hamilton wedge/cyanuric acid) as well as the B21C7–AS host–guest system, was designed. The diblock copolymer was unfolded by the addition of KPF_6 as a competitive guest for the B21C7 moiety. The dual-gated unfolding of the single-chain folded nanostructures based on the tetrablock copolymer was induced by 1) the addition of methanol to disrupt the hydrogen bonds and consecutive decomplexation of the host–guest motif by addition of KPF_6 and 2) decomplexation of the B21C7–AS host–guest motif and the subsequent cleavage of the hydrogen bonds by addition of methanol. The unfolding of the host–guest motif in the diblock copolymer as well as the stepwise unfolding of the tetrablock copolymer are evidenced by dynamic light scattering and diffusion-ordered spectroscopy data. The introduced dual-gated SCNP unfolding system marks a significant step forward in designing dynamic SCNP systems that are able to be orthogonally addressed in their response to outer stimuli. We envision that the current study will spur efforts to design even higher order gated unfolding systems, also including those triggered by outer fields, including photonic and magnetic fields.

Acknowledgements

C.B.-K. and B.L. acknowledge funding for this project by the Sonderforschungsbereich 1176, project A1, of the German Research Council (DFG). C.B.-K. and B.L. also acknowledge long-term funding by the Helmholtz Association in the context of the Biointerfaces in Technology and Medicine (BIFTM) program. NMR measurements were performed in the DFG instrumentation facility Pro^{2}NMR.

Keywords: host–guest interactions · orthogonal unfolding · polymer synthesis · single-chain folding · supramolecular chemistry

How to cite: *Angew. Chem. Int. Ed.* **2016**, *55*, 11276–11280
Angew. Chem. **2016**, *128*, 11446–11450

[1] C. B. Anfinsen, *Science* **1973**, *181*, 223–230.
[2] C. M. Dobson, *Nature* **2003**, *426*, 884–890.
[3] O. Altintas, P. Krolla-Sidenstein, H. Gliemann, C. Barner-Kowollik, *Macromolecules* **2014**, *47*, 5877–5888.
[4] N. Hosono, M. A. J. Gillissen, Y. Li, S. S. Sheiko, A. R. A. Palmans, E. W. Meijer, *J. Am. Chem. Soc.* **2013**, *135*, 501–510.
[5] D. J. Hill, M. J. Mio, R. B. Prince, T. S. Hughes, J. S. Moore, *Chem. Rev.* **2001**, *101*, 3893–4011.
[6] V. W. Kuhn, H. Majer, *Makromol. Chem.* **1956**, *18*, 239–253.
[7] B. D. Mecerreyes, V. Lee, C. J. Hawker, J. L. Hedrick, A. Wursch, W. Volksen, T. Magbitang, E. Huang, R. D. Miller, *Adv. Mater.* **2001**, *13*, 204–208.
[8] M. Gonzalez-Burgos, A. Latorre-Sanchez, J. A. Pomposo, *Chem. Soc. Rev.* **2015**, *44*, 6122–6142.
[9] a) O. Altintas, C. Barner-Kowollik, *Macromol. Rapid Commun.* **2012**, *33*, 958–971; b) O. Altintas, C. Barner-Kowollik, *Macromol. Rapid Commun.* **2016**, *37*, 29–46.
[10] A. M. Hanlon, C. K. Lyon, E. B. Berda, *Macromolecules* **2016**, *49*, 2–14.
[11] C. K. Lyon, A. Prasher, A. M. Hanlon, B. T. Tuten, C. A. Tooley, P. G. Frank, E. B. Berda, *Polym. Chem.* **2015**, *6*, 181–197.
[12] S. Mavila, O. Eivgi, I. Berkovich, N. G. Lemcoff, *Chem. Rev.* **2016**, *116*, 878–961.
[13] W. A. Braunecker, K. Matyjaszewski, *Prog. Polym. Sci.* **2007**, *32*, 93–146.

[14] M. Ouchi, N. Badi, J.-F. Lutz, M. Sawamoto, *Nat. Chem.* **2011**, *3*, 917 – 924.
[15] R. K. Roy, J.-F. Lutz, *J. Am. Chem. Soc.* **2014**, *136*, 12888 – 12891.
[16] C. F. Hansell, A. Lu, J. P. Patterson, R. K. O'Reilly, *Nanoscale* **2014**, *6*, 4102 – 4107.
[17] T. Mes, R. Van Der Weegen, A. R. A. Palmans, E. W. Meijer, *Angew. Chem. Int. Ed.* **2011**, *50*, 5085 – 5089; *Angew. Chem.* **2011**, *123*, 5191 – 5195.
[18] O. Altintas, P. Gerstel, N. Dingenouts, C. Barner-Kowollik, *Chem. Commun.* **2010**, *46*, 6291 – 6293.
[19] E. B. Berda, E. J. Foster, E. W. Meijer, *Macromolecules* **2010**, *43*, 1430 – 1437.
[20] J. Lu, N. Ten Brummelhuis, M. Weck, *Chem. Commun.* **2014**, *50*, 6225 – 6227.
[21] E. A. Appel, J. Dyson, J. Delbarrio, Z. Walsh, O. A. Scherman, *Angew. Chem. Int. Ed.* **2012**, *51*, 4185 – 4189; *Angew. Chem.* **2012**, *124*, 4261 – 4265.
[22] J. Willenbacher, B. V. K. J. Schmidt, D. Schulze-Suenninghausen, O. Altintas, B. Luy, G. Delaittre, C. Barner-Kowollik, *Chem. Commun.* **2014**, *50*, 7056 – 7059.
[23] A. Sanchez-Sanchez, A. Arbe, J. Colmenero, J. A. Pomposo, *ACS Macro Lett.* **2014**, *3*, 439 – 443.
[24] J. Willenbacher, O. Altintas, V. Trouillet, N. Knöfel, M. J. Monteiro, P. W. Roesky, C. Barner-Kowollik, *Polym. Chem.* **2015**, *6*, 4358 – 4365.
[25] N. Hosono, A. M. Kushner, J. Chung, A. R. A. Palmans, Z. Guan, E. W. Meijer, *J. Am. Chem. Soc.* **2015**, *137*, 6880 – 6888.
[26] Z. Yang, Y. Shi, W. Chen, F. Wang, *Polym. Chem.* **2015**, *6*, 5540 – 5544.
[27] O. Altintas, M. Artar, G. Ter Huurne, I. K. Voets, A. R. A. Palmans, C. Barner-Kowollik, E. W. Meijer, *Macromolecules* **2015**, *48*, 8921 – 8932.
[28] V. V. Rostovtsev, L. G. Green, V. V. Fokin, K. B. Sharpless, *Angew. Chem. Int. Ed.* **2002**, *41*, 2596 – 2599; *Angew. Chem.* **2002**, *114*, 2708 – 2711.
[29] S. Dong, Y. Luo, X. Yan, B. Zheng, X. Ding, Y. Yu, Z. Ma, Q. Zhao, F. Huang, *Angew. Chem. Int. Ed.* **2011**, *50*, 1905 – 1909; *Angew. Chem.* **2011**, *123*, 1945 – 1949.
[30] B. Neises, W. Steglich, *Angew. Chem. Int. Ed. Engl.* **1978**, *17*, 522 – 524; *Angew. Chem.* **1978**, *90*, 556 – 557.
[31] Y. Liu, Z. Wang, X. Zhang, *Chem. Soc. Rev.* **2012**, *41*, 5922 – 5932.
[32] M. Zhang, D. Xu, X. Yan, J. Chen, S. Dong, B. Zheng, F. Huang, *Angew. Chem. Int. Ed.* **2012**, *51*, 7011 – 7015; *Angew. Chem.* **2012**, *124*, 7117 – 7121.
[33] L. Chen, Y. K. Tian, Y. Ding, Y. J. Tian, F. Wang, *Macromolecules* **2012**, *45*, 8412 – 8419.
[34] O. Altintas, E. Lejeune, P. Gerstel, C. Barner-Kowollik, *Polym. Chem.* **2012**, *3*, 640 – 651.

Received: March 23, 2016
Revised: May 10, 2016
Published online: June 30, 2016

